ACTIVE HAIR-BUNDLE MOTILITY BY THE VERTEBRATE HAIR CELL

J-Y. TINEVEZ[†], P. MARTIN

Laboratoire Physico-Chimie Curie, CNRS, Institut Curie, UPMC
26, rue d'Ulm, F- 75248 Paris cedex 05, France

F. JÜLICHER

Max-Planck-Institute for the Physics of Complex Systems
Nöthnitzer Str. 38, 01187 Dresden, Germany

The hair bundle is both a mechano-sensory antenna and a force generator that might help the vertebrate hair cell from the inner ear to amplify its responsiveness to small stimuli. To study active hair-bundle motility, we combined calcium iontophoresis with mechanical stimulation of single hair bundles from the bullfrog's sacculus. A hair bundle could oscillate spontaneously, or be quiescent but display non-monotonic movements in response to abrupt force steps. Extracellular calcium changes or static biases to the bundle's position at rest could affect the kinetics of bundle motion and evoke transitions between the different classes of motility. The calcium-dependent location of a bundle's operating point within its nonlinear force-displacement relation controlled the type of movements observed. A unified theoretical description, in which mechanical activity stems from myosin-based adaptation and electro-mechanical feedback by Ca^{2+}, could account for the fast and slow manifestations of active hair-bundle motility.

1 Introduction

Sensory hair cells in the inner ear make use of mechanical amplification to enhance their sensitivity and sharpen their frequency selectivity to faint stimuli [1]. The mechanism that would explain this active process remains a central issue of auditory biophysics. In the mammalian ear, somatic electromotility of outer hair cells [2] appears to be necessary for cochlear amplification [3; 4] but its exact contribution to the cochlear amplifier is still under debate [5]. Non-mammalian hair cells lack electromotility but nevertheless display sensitive and frequency selective hearing [6]. There, the motor of the amplificatory process most probably resides in the hair bundle, the tuft of extended actin-rich microvilli that adorns the apical surface of each hair cell.

Spontaneous hair-bundle oscillations demonstrate that a hair cell can power movements of its mechano-sensory organelle, even in the absence of stimulation (reviewed in [7]). Moreover, active oscillations provide a characteristic frequency near which a hair bundle displays increased sensitivity to small periodic mechanical stimuli [8; 9]. Other forms of activity have been reported under conditions for which hair bundles are quiescent. When stimulated by an abrupt force step with a flexible glass fiber, a hair bundle can indeed produce a non-monotonic "twitch" in which motion in the direction of

[†] Jean-Yves Tinevez's present address is Max-Plank-Institute of Molecular Cell Biology and Genetics, Pfötenhauerstrasse 108, 01307 Dresden Germany.

the applied force is interrupted by a fast recoil [10-12]. In other cases, the hair bundle monotonically relaxes towards a new steady state position that can sometimes exceed that of the stimulus fiber's base [13]. These various regimes of hair-bundle motility are intimately related to adaptation, the active process that provides negative feedback on the open probability of the transduction channels. We review here recent evidence [14] that clarify the role of gating compliance, the mechanical correlate of channel gating, and of the Ca^{2+} component of the transduction current in shaping the type of active movements that a hair bundle can produce. By so doing, we provide a minimal and unified physical description of active hair-bundle motility.

2 Methods

2.1 Mechanical stimulation of single hair bundles and Ca^{2+} iontophoresis

Each experiment was performed at a room temperature of 21-24 °C with hair cells from the saccule of an adult bullfrog (*Rana catesbeiana*) by published methods [14]. In short, the preparation was mounted on a two-compartment chamber. While the basolateral surface was bathed by standard saline consisting of 110 mM Na^+, 2 mM K^+, 4 mM Ca^{2+}, 122 mM Cl^-, 3 mM **D**-glucose, 2 mM creatine phosphate, 2 mM sodium pyruvate and 5 mM HEPES, hair bundles projected in NMDG artificial endolymph containing 2 mM Na^+, 3 mM K^+, 0.075-4 mM Ca^{2+}, 110 mM *N*-methyl-**D**-glucamine, 111 mM Cl^-, 3 mM **D**-glucose, and 5 mM HEPES. After digestion with the protease subtilisin (Sigma, type XXIV) at a concentration of 50-67 $\mu g \cdot ml^{-1}$ in endolymph for 25 mn, the otolithic membrane was peeled off the macula to get access to individual hair bundles. Each solution had a pH of ~7.3 and an osmotic strength of ~230 $mmol \cdot kg^{-1}$.

The experimental chamber was secured to the stage of an upright microscope (BX51WI, Olympus). The preparation was viewed using bright-field illumination through a ×60 water-immersion objective lens and a ×1.25 relay lens. The tip of a hair bundle, or of a stimulus fiber attached to it, was imaged at a magnification of ×1,000 on a displacement monitor which included a dual photodiode (PIN-SPOT2D, UDT Sensor Inc.). This photometric system was characterized by a bandwidth of 6.5 kHz at half the maximal power and yielded an output linearly proportional to the displacement of the stimulus fiber in a range of ±500 nm with a resolution of ~1 µm, corresponding to a ~1 nm resolution at the specimen plane.

Hair-bundles were stimulated with flexible glass fibers that were fabricated from borosilicate capillaries and coated with a ~100 nm layer of gold-palladium to enhance optical contrast [15]. The stiffness K_F and drag coefficient λ_F of the fibers were respectively, 150-500 $\mu N \cdot m^{-1}$ and 40-200 $nN \cdot s \cdot m^{-1}$. The fiber was secured by its base to a stack-type piezoelectric actuator (PA 8/14, Piezosystem Jena) driven by a low-noise power supply (ENV 150 and ENT 150/20, Piezosystem Jena). When powered by an unfiltered, abrupt voltage step, the actuator with an attached rigid fiber displayed a mechanical resonance at ~4 kHz. By using displacement-clamp circuitry to apply a series of step displacements to a hair-bundle, we measured the forces that had to be exerted to

hold the hair bundle at these positions, thereby describing the intrinsic force-displacement relation of the hair bundle [15; 16]. For each displacement step, we estimated the elastic response of the hair bundle by recording the force ~3 ms after the onset of stimulation to allow just enough time for the viscous response to vanish and minimize the mechanical relaxation provided by adaptation [16].

We used iontophoresis to rapidly change the local Ca^{2+} concentration near a hair bundle. Coarse microelectrodes were fabricated from borosilicate capillaries, bent through an angle of ~90° in their tapered region and then filled either with 2.5 M $CaCl_2$ or 350 mM disodium ATP (here used as a Ca^{2+} chelator). At a distance $r = 3$ µm from the hair bundle, this technique allowed an increase of ~20 µM of Ca^{2+} concentration per nanoampere of iontophoretic current.

2.2 Theoretical description of active hair-bundle mechanics

This description (detailed in [7; 14]) is based on the gating-spring theory of mechano-electrical transduction [17] and a myosin-based model of adaptation [18; 19].

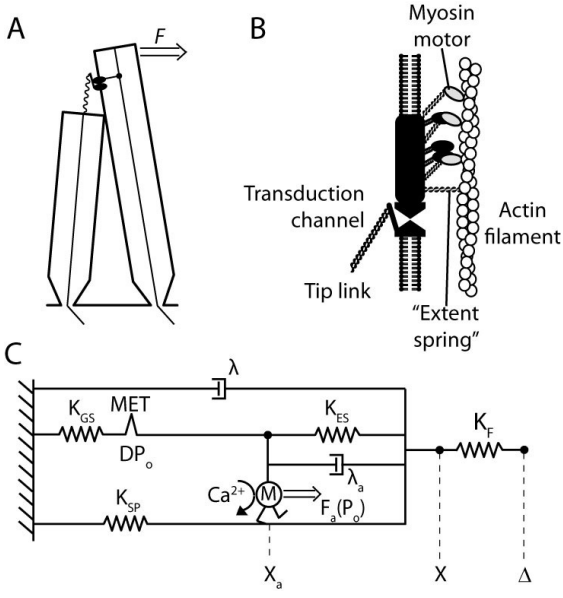

Figure 1. A: Schematic representation of a hair bundle. We assumed that N transduction elements, here lumped into a single element, operate in parallel within a hair bundle. An external force F is applied to the tip of the hair bundle and defined positive when oriented as depicted here. B: Functional view of a transduction element (adapted from [18]). At steady state, the active force exerted towards the tip of the stereocilia by a group of ~60 myosin molecules is balanced by an elastic restoring tension in the tip link, thereby defining the resting open probability of the mechano-sensitive transduction channel. C: Mechanical arrangement. Transduction channels (MET) of open probability P_o are connected to gating springs of stiffness K_{GS} and anchored to the actin cytoskeleton of the stereocilia, dynamically by adaptation motors (M) that can change their position X_a and statically by extent springs of stiffness K_{ES} that limit the extent of adaptive movements of the motors. The external force $F = K_F(\Delta - X)$, exerted by means of a flexible fiber of stiffness K_F, affects tension in both gating and pivot springs, the later being of stiffness K_{SP} and operating in parallel to the former. The speed of hair-bundle motion is inversely proportional to the friction coefficient λ. Opening of a transduction channel evokes a decrease of gating-spring extension that amounts to a motion of size D of the bundle's top [17]. When the combined tension in gating and extent springs differs from the active force F_a that the adaptation motors produce at stall, the motors are moving. Motor speed is inversely proportional to λ_a, which has units of a friction coefficient and represents the slope of the force-velocity relation of the motors near stall condition. The motor force F_a is down-regulated by the Ca^{2+} concentration at the motor site and thus depends on P_o. All variables are expressed at the top of a hair bundle along the stimulation axis.

The dynamic interplay between the positions X of the hair bundle and X_a of the adaptation motor (Fig. 1) is described by two coupled equations:

$$\lambda \frac{dX}{dt} = -\mathrm{K}_{GS}\left(X - X_a - D\,P_o\right) - \mathrm{K}_{SP}X + F \tag{1}$$

$$\lambda_a \frac{dX_a}{dt} = \mathrm{K}_{GS}\left(X - X_a - D\,P_o\right) - \mathrm{K}_{ES}\left(X_a - X_{ES}\right) - F_a\,, \tag{2}$$

in which the open probability of the transduction channels is given by:

$$P_o = \frac{1}{1 + A\exp\left(-\dfrac{Z\left(X - X_a\right)}{k_B T}\right)}. \tag{3}$$

Here, X_{ES} is the value of X_a for which the extent springs bear no tension, $P_o = 1/(1+A)$ when the gating springs are severed and $Z = \mathrm{K}_{GS}\,D/N$ is the gating force of a single transduction element.

To account for the regulation of adaptation by Ca^{2+} [20; 21], we assumed here that the only effect of Ca^{2+} was to down-regulate the active force F_a produced by the motors at stall. By demonstrating that the ATPase cycle of myosin-1c, the putative adaption motor [23], is regulated by Ca^{2+}, recent biochemical evidence in vitro [22] provided support for this assumption. For simplicity, we further supposed that F_a depends instantaneously and linearly on the Ca^{2+} concentration at the motor site and that this concentration equilibrates within microseconds of channel gating. These assumptions yield the relation:

$$F_a \cong F_{\max}\left(1 - S\,P_o\right), \tag{4}$$

in which $F_{\max}$ is the maximal force that the motors can generate at stall and the dimensionless parameter S defines the strength of the Ca^{2+} feedback on the motor force. Note that S is proportional to the extracellular Ca^{2+} concentration, which could be modified experimentally.

3 Results

3.1 Three classes of active hair-bundle movements

A hair bundle could be quiescent but display non-monotonic movements in response to step stimuli that were either negatively or positively directed, but not both (Fig 2A and C, respectively; see also Fig 3). These “twitches” were associated with force-displacement relations in which linear branches for large positive or negative displacements were separated by a region of reduced slope near the position that the hair bundle assumed at rest. Interestingly, this operating point lay on one side of the compliant region of the force-displacement relation. Correspondingly, twitches were observed only when the external stimulus had the appropriate directionality to force the hair bundle to explore the

nonlinear region of its force-displacement relation. A hair bundle could also oscillate spontaneously (Fig 2B). As recognized before [16], this active behavior was associated with an intrinsic force-displacement relation containing a region of negative slope and an operating point located within this unstable region. It was thus possible to classify active hair-bundle movements in three categories according to the properties of the intrinsic force-displacement relation of the corresponding hair bundles.

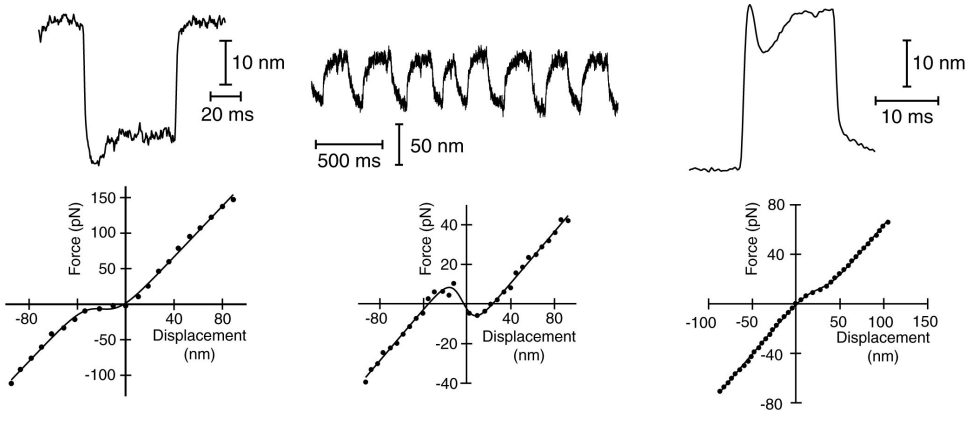

Figure 2. Active hair-bundle movements. A: Negative twitch elicited by a -60 nm step displacement of the stimulus fiber's base. The fiber had a stiffness of K_F = 739 µm/N. B: Spontaneous oscillations of hair-bundle position at ~12 Hz with a peak-to-peak magnitude of 63 nm. C: Positive twitch in response to a +137 nm displacement of the fiber's base (K_F = 270 µm/N). Note the difference in kinetics between positive (fast) and negative (slow) twitches. Each hair bundle was characterized by a force-displacement relation that is shown below the corresponding active behavior. The Ca^{2+} concentration in the fluid bathing the hair bundle was 250 µM in (A) and (B), and 4 mM in (C).

3.2 Ca^{2+} involvement in active hair-bundle motility

Spontaneous oscillations were most often observed under two-compartment ionic conditions that mimicked native physiological conditions with 250 µM Ca^{2+} in endolymph, whereas positive and negative twitches were favored by high and low Ca^{2+} concentrations, respectively. Extracellular Ca^{2+} changes are known to affect the kinetics of active hair-bundle movements [11; 14; 15]. Higher Ca^{2+} concentrations indeed result in sharper twitches or faster spontaneous oscillations, whereas reduced Ca^{2+} concentration result in slower active movements. For large enough Ca^{2+} changes, we could evoke, with the same hair bundle, transitions between the three classes of active hair-bundle motility (Fig. 3A-D). Our classification of active hair-bundle movements (Fig. 2) suggests that these transitions should be associated with a shift of the corresponding force-displacement relation. By using Ca^{2+} iontophoresis, we could indeed demonstrate that increased Ca^{2+} concentrations evoked a positively-directed shift of the force-displacement relation of a given hair bundle (Fig. 3E). The converse behavior was also observed (not shown).

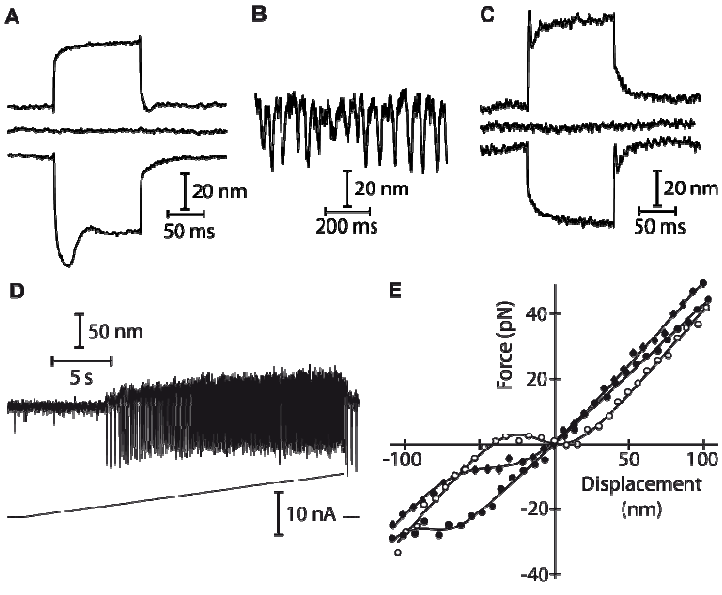

Figure 3. Effects of Ca^{2+} on hair-bundle motitily. A-C: A quiescent hair bundle that displayed a negative twitch when exposed to 75 µM Ca^{2+} (A) could also show spontaneous oscillations under the same conditions (B) but produced a positive twitch (C) when subjected to 4 mM Ca^{2+}. D: Another hair bundle was quiescent at rest but became oscillatory when iontophoresis was used to increase the Ca^{2+} concentration in its vicinity (ramp of iontophoretic current shown at the bottom). The oscillation frequency almost tripled from ~4 Hz to ~11 Hz, whereas the amplitude of the negatively-directed spikes remained roughly constant at ~100 nm. This hair bundle was characterized by a force-displacement relation that resembled that shown in Fig. 2C. E: Measurement of the force-displacement relation for increasing iontophoretic currents (●: -5 nA, holding current; ♦: +3 nA; ○: +6 nA) revealed a positively-directed shift. Although the hair bundle was stable under control conditions (●), the bundle's operating point belonged to an unstable region of negative stiffness of the force-displacement relation for an iontophoretic current of +6 nA (○). Under such circumstances, the hair bundle oscillated spontaneously (not shown).

Calcium changes not only affected the operating point of a hair bundle within its intrinsic force-displacement relation (Fig. 3E) but also evoked net movements. In the case of non-oscillatory hair bundles, we studied the time course of Ca^{2+}evoked movements by using iontophoresis of Ca^{2+} or of a Ca^{2+} chelator [14]. Notably, the directionality of a Ca^{2+} evoked movement varied from cell to cell within the same epithelium and could even be non-monotonic. Moreover, the directionality of bundle movement could be reversed by imposing an offset to the resting position of the hair bundle before applying the iontophoretic pulse (Fig. 4). Polarity reversal of Ca^{2+}-evoked movements was associated with a change in kinetics: for a given Ca^{2+} change, movements in one direction were always slower than when they occurred in the opposite direction.

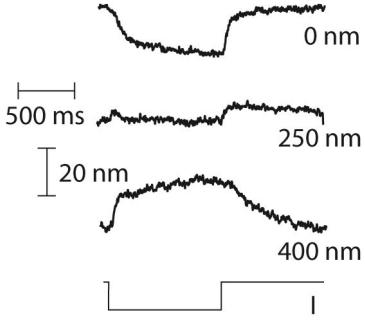

Figure 4. Ca^{2+} evoked movements at various resting positions of a quiescent hair bundle. In response to an iontophoretic pulse of a Ca^{2+} chelator (I = -50 nA; shown at the bottom), here ATP, this quiescent hair bundle displayed a slow movement in the negative direction. With a +250 nm bias, the same hair bundle produced a small biphasic motion with no net deflection at steady state. In the presence of larger biases, here +400 nm, the ATP-evoked movement displayed faster kinetics and opposite directionality than those measured with no offset. The hair bundle was immersed in artificial endolymph containing 250µM Ca^{2+}.

3.3 Simulations

Numerically solving the dynamic Eqs. 1 and 2 for the position X of the hair-bundle and X_a of the adaptation motor, together with Eq. 4 that describes Ca^{2+} feedback on the motor's activity, we could mimic the three classes of active hair-bundle movements that we have observed in the bullfrog (Fig. 5) as well as Ca^{2+}-evoked movements (not shown) [14].

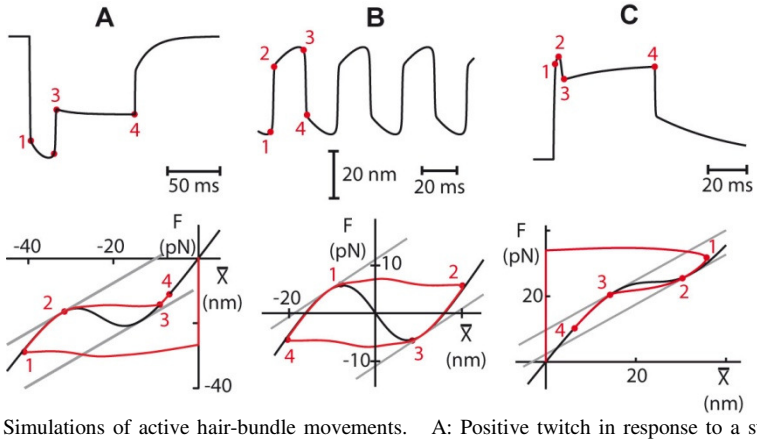

Figure 5. Simulations of active hair-bundle movements. A: Positive twitch in response to a step force of +35 pN. B: Spontaneous oscillations. C: Negative twitch in response to a force step of -30 pN. In each case, we enforced a force-displacement relation, shown at below each type of movement, and an operating point within this relation that resembled those we measured (Fig. 2), thereby constraining most parameters (see reference [14] for parameter values). The trajectory superimposed on each force-displacement relation represents the force $F - K_{SP}\overline{X}_a$ as a function of $\overline{X} - \overline{X}_a$, in which $\overline{X}$ and $\overline{X}_a$ are the hair-bundle and motor positions, respectively, with respect to their steady-state values. The grey oblique lines have a slope of K_{SP}, the stiffness of the stereociliary pivots.

4 Discussion

Linear-stability analysis of the dynamical system defined by Eqs. 1 and 2 indicates that the hair bundle can become oscillatory if two necessary conditions are met. First, gating compliance must be strong enough that the force-displacement relation displays a region bundle positions for which the slope stiffness $K_{HB} = \overline{K}_{GS} + K_{SP}$ of the system is

negative: the apparent gating-spring stiffness $\overline{\mathrm{K}}_{GS} = \mathrm{K}_{GS}\left(1-\left(ZDP_o\left(1-P_o\right)\right)/\left(k_BT\right)\right)$ must be negative enough to dominate the pivot stiffness K_{SP}. Second, the Ca^{2+}-feedback strength S must be neither too large nor too small in order to position the system's operating point within the unstable region of negative stiffness. In such instance, the myosin-based adaptation motor can never reach stall condition and thus produces an oscillation (Fig. 5B). Note that without Ca^{2+} feedback, the system is always stable, even in the presence of negative stiffness. When operating on the verge of an unstable region of negative stiffness, however, the system is excitable: pushed across the unstable region of negative stiffness by an external force, the system relaxes back towards its operating point by displaying a non-monotonic twitch-like movement whose time-course looks like one half-cycle of a spontaneous oscillation (Fig. 5A).

When $\mathrm{K}_{HB}>0$, the system is stable but can nevertheless display twitches in response to abrupt step forces (Fig. 5C). In the limit where hair-bundle motion is fast compared to motor movements, Eq. 1 indeed indicates that an adaptive movement of the motor elicits a movement of the hair bundle that can be approximated by:

$$\delta X = \frac{\overline{\mathrm{K}}_{GS}}{\mathrm{K}_{HB}}\,\delta X_a \,. \tag{5}$$

A positive adaptive movement of the motor towards the base of the stereocilia, as would be expected in response to a positive force step or to a sudden increase of the extracellular Ca^{2+} concentration, can thus evoke a negative deflection of the hair bundle (a recoil), provided that $\overline{\mathrm{K}}_{GS}$ or equivalently that the hair-bundle stiffness is locally smaller than that of the stereociliary pivots. This condition can be met only if gating-compliance is strong enough that $ZD > 4k_BT$ and, if the case, is more easily met near $P_o = 0.5$ where the mechanical effects of channel gating are the greatest. Note that in contrast to movements of the adaptation motors, the internal forces that result from the conformational changes associated to channel gating during adaptation provide positive feedback on gating-spring tension. Non-monotonic movements are the result of a non-linear and dynamic tradeoff between opposing forces that are produced by adaptation motors on one end and those exerted by adaptive channel gating on the other end.

The kinetics of active hair-bundle movements and of the associated transduction currents (Eq. 3) are controlled in part by how fast the adaptation motors can react to an external perturbation. Adaptation kinetics can easily be discussed in the simple case where the bundle's position is clamped and a small step displacement δX is applied. Then, Eq. 2 indicates that the time-course of the adaptive shift δX_a can be described by a single exponential with the characteristic timescale

$$\tau_a = \lambda_a \Big/ \left(\tilde{\mathrm{K}}_{GS} + \mathrm{K}_{ES}\right) \,. \tag{6}$$

in which the effective gating-spring stiffness $\tilde{\mathrm{K}}_{GS}$ is given by:

$$\tilde{\mathrm{K}}_{GS} = \mathrm{K}_{GS}\left(1-\frac{ZD}{k_BT}\left(1-S\,\frac{F_{\max}}{\mathrm{K}_{GS}D}\right)P_o\left(1-P_o\right)\right) \,. \tag{7}$$

In the case where Ca^{2+} feedback is strong enough that $S > K_{GS} D / F_{max}$, intracellular Ca^{2+} changes that result from channel gating effectively stiffen the gating springs ($\tilde{K}_{GS} > K_{GS}$), thereby providing an effect opposite that of gating compliance. Adaptation is thus expected to be significantly faster when the system operates near $P_o = 0.5$ than near $P_o = 0$ or 1, where the stimulus evokes little channel rearrangements. With parameters appropriate for transduction in the bullfrog sacculus [14], fast and slow adaptations are characterized by timescale of 4 and 24 ms, respectively. Because S is proportional to the extracellular Ca^{2+} concentration, fast adaptation will occur preferentially at high Ca^{2+}. At low Ca^{2+} concentrations, Ca^{2+} feedback on the motor force is too weak to fully overcome the effects of gating compliance ($\tilde{K}_{GS} < K_{GS}$), and adaptation is thus always slow, reaching timescales of several tens of milliseconds or more near $P_o = 0.5$.

Because adaptation is incomplete, a static deflection of the hair bundle can displace the bundle's operating point within its force-displacement relation and, correspondingly, change the open probability of the transduction channels at steady state. By so doing, the directionality of active hair-bundle movements evoked by a given stimulus can be inverted and its kinetics altered, as we have observed experimentally (Fig. 4). These effects can be described by a change in sign of $\overline{K}_{GS}$ and in magnitude of $\tilde{K}_{GS}$, respectively.

In conclusion, only three ingredients suffice to account for the different manifestations of active hair-bundle motility: strong gating-compliance, myosin-based adaptation and Ca^{2+} feedback on the motor's activity.

Acknowledgments

J.-Y.T. and P.M. supported by HFSP grant RGP0051/2003 and by European Commission FP6 Integrated Project EUROHEAR, LSHG-CT-2004-512063.

References

1. Hudspeth, A.J. 1997. Mechanical amplification of stimuli by hair cells. Curr. Opin. Neurobiol. 7, 480-486.
2. Santos-Sacchi, J. 2003. New tunes from Corti's organ: the outer hair cell boogie rules. Curr Opin Neurobiol 13, 459-68.
3. Dallos, P., Wu, X., Cheatham, M.A., Gao, J., Zheng, J., Anderson, C.T., Jia, S., Wang, X., Cheng, W.H., Sengupta, S., He, D.Z., Zuo, J. 2008. Prestin-based outer hair cell motility is necessary for mammalian cochlear amplification. Neuron 58, 333-9.
4. Mellado Lagarde, M.M., Drexl, M., Lukashkina, V.A., Lukashkin, A.N., Russell, I.J. 2008. Outer hair cell somatic, not hair bundle, motility is the basis of the cochlear amplifier. Nat Neurosci 11, 746-8.
5. Chan, D.K., Hudspeth, A.J. 2005. Ca2+ current-driven nonlinear amplification by the mammalian cochlea in vitro. Nat. Neurosci. 8, 149-55.
6. Manley, G.A. 2001. Evidence for an active process and a cochlear amplifier in nonmammals. J. Neurophysiol. 86, 541-549.

7. Martin, P. 2008. Active hair-bundle motility of the hair cells of vestibular and auditory organs. In: Manley, G.A., Popper, A.N., Fay, R.R., (Eds.), Active processes and otoacoustic emissions. Springer, New York. pp. 93-144.
8. Martin, P., Hudspeth, A.J. 2001. Compressive nonlinearity in the hair bundle's active response to mechanical stimulation. Proc. Natl. Acad. Sci. USA 98, 14386-14391.
9. Martin, P., Hudspeth, A.J. 1999. Active hair-bundle movements can amplify a hair cell's response to oscillatory mechanical stimuli. Proc. Natl. Acad. Sci. USA 96, 14306-14311.
10. Howard, J., Hudspeth, A.J. 1987. Mechanical relaxation of the hair bundle mediates adaptation in mechanoelectrical transduction by the bullfrog's saccular hair cell. Proc. Natl. Acad. Sci. USA 84, 3064-3068.
11. Ricci, A.J., Crawford, A.C., Fettiplace, R. 2000. Active hair bundle motion linked to fast transducer adaptation in auditory hair cells. J. Neurosci. 20, 7131-7142.
12. Benser, M.E., Marquis, R.E., Hudspeth, A.J. 1996. Rapid, active hair bundle movements in hair cells from the bullfrog's sacculus. J. Neurosci. 16, 5629-5643.
13. Kennedy, H.J., Crawford, A.C., Fettiplace, R. 2005. Force generation by mammalian hair bundles supports a role in cochlear amplification. Nature 433, 880-3.
14. Tinevez, J.Y., Julicher, F., Martin, P. 2007. Unifying the various incarnations of active hair-bundle motility by the vertebrate hair cell. Biophys J 93, 4053-67.
15. Martin, P., Bozovic, D., Choe, Y., Hudspeth, A.J. 2003. Spontaneous oscillation by hair bundles of the bullfrog's sacculus. J. Neurosci. 23, 4533-48.
16. Martin, P., Mehta, A.D., Hudspeth, A.J. 2000. Negative hair-bundle stiffness betrays a mechanism for mechanical amplification by the hair cell. Proc. Natl. Acad. Sci. USA 97, 12026-12031.
17. Howard, J., Hudspeth, A.J. 1988. Compliance of the hair bundle associated with gating of mechanoelectrical transduction channels in the bullfrog's saccular hair cell. Neuron 1, 189-199.
18. Hudspeth, A.J., Gillespie, P.G. 1994. Pulling springs to tune transduction: adaptation by hair cells. Neuron 12, 1-9.
19. Assad, J.A., Corey, D.P. 1992. An active motor model for adaptation by vertebrate hair cells. J. Neurosci. 12, 3291-309.
20. Hacohen, N., Assad, J.A., Smith, W.J., Corey, D.P. 1989. Regulation of tension on hair-cell transduction channels: displacement and calcium dependence. J. Neurosci. 9, 3988-3997.
21. Crawford, A.C., Evans, M.G., Fettiplace, R. 1991. The actions of calcium on the mechano-electrical transducer current of turtle hair cells. J. Physiol. 434, 369-398.
22. Adamek, N., Coluccio, L.M., Geeves, M.A. 2008. Calcium sensitivity of the cross-bridge cycle of Myo1c, the adaptation motor in the inner ear. Proc Natl Acad Sci U S A 105, 5710-5.
23. Stauffer, E.A., Scarborough, J.D., Hirono, M., Miller, E.D., Shah, K., Mercer, J.A., Holt, J.R., Gillespie, P.G. 2005. Fast adaptation in vestibular hair cells requires Myosin-1c activity. Neuron 47, 541-53.